Alkaline Hydrolysis of Amide Bonds: Effect of Bond Twist and Nitrogen Pyramidalization

Xabier Lopez,[†] Jon Iñaki Mujika,[†] G. Michael Blackburn,[‡] and Martin Karplus*[,§,||]

Kimika Fakultatea, Euskal Herriko Unibertsitatea, P.K. 1072, 20080 Donostia, Euskadi, Spain, Department of Chemistry, The University of Sheffield, Sheffield S3 7HF, England, Laboratoire de Chimie Biophysique, Institut le Bel, Université Louis Pasteur, 67000 Strasbourg, France, and Department of Chemistry and Chemical Biology, Harvard University, Cambridge, Massachusetts 02138

Received: September 6, 2002; In Final Form: January 17, 2003

We present an ab initio study of the alkaline hydrolysis reaction of planar and pyramidal amides. The aim is to investigate the effect of C−N bond twisting and nitrogen pyramidalization on the rate of hydrolysis. The transition states, intermediates, and products for the two steps of the reaction (hydroxide attack and breaking of the C−N bond) were characterized in the gas phase using the B3LYP density functional quantum mechanical method with the 6-31+G* basis set. The energetics were then refined using the 6-311++G(d,p) basis set. The effect of the solvent was introduced by means of several methods: Poisson−Boltzmann (PB) and polarizable continuum model (PCM) calculations at the gas-phase geometries; both allow for charge relaxation in solution. We found that the transition state corresponding to the second step of the reaction (TS2), breaking of the C−N bond, is the transition state of highest energy in the gas phase and in solution. However, calculation with formamide as a model showed that the inclusion of an explicit water molecule significantly decreases the TS2 barrier. The $\Delta\Delta G^{TS2}$ between the twisted and planar species is about 15 kcal/mol in solution, favoring the hydrolysis of the former. Our estimation for the value of the $\Delta\Delta G^{TS1}$ for the first step of the reaction, hydroxide addition, ranges between 7 and 9.7 kcal/mol. There are also significant differences between the planar and twisted forms in the thermodynamics of the reaction. In solution, the hydrolysis of the twisted amide is exothermic by −6.8 kcal/mol, whereas the hydrolysis of the planar amide is highly endothermic, 16 kcal/mol. Thus, twisting of the amide bond and nitrogen pyramidalization is found to be an effective way of accelerating the otherwise slow hydrolysis of planar amides. As much as 14.7 kcal/mol of acceleration could be expected if the rate-limiting transition state is the breaking of the C−N bond from the tetrahedral intermediate, and 7.0−9.7 kcal/mol could be expected if the rate-limiting step is hydroxide attack. The fact that experimental studies have demonstrated a rate enhancement of about 10 kcal/mol suggests that the latter step is rate-limiting in alkaline solution.

1. Introduction

The amide bond is of fundamental importance in biology as the essential element of the protein backbone. The hydrolysis reaction of amides, often used as a model for the cleavage of peptide bonds,[1,2] is thus of primary concern for living systems. Unactivated amides undergo very slow hydrolysis in neutral media. The half-life for the hydrolysis of acetyl-glycil-glycine is 500 years[3] at pH 6.8 and 25 °C, and the calculated free-energy barrier for the reaction of a water molecule with formamide is 44.0 kcal/mol at the MP2/6-31G*//3-21G level of theory.[4] Alkaline hydrolysis of formamide has a lower barrier; a thermodynamic analysis by Guthrie[5] suggests an effective $\Delta G^{\neq}$ of 22.0 kcal/mol. The first step of the reaction involves the formation of a tetrahedral intermediate and pyramidalization at the amide nitrogen. Thus, distortion of the nitrogen from its planar ground state could accelerate the rate of hydrolysis. Early kinetic work[6,7] showed that pyramidalization of the amide nitrogen by the use of benzoquinuclidin-2-one, a strained cyclic amide, leads to alkaline hydrolysis that is 10^7 times faster than its strainless counterpart. This correspond to a decrease in the activation energy of the reaction by about 10 kcal/mol. Brown et al. also reported[2,8] significant accelerations for the hydrolysis of distorted amides, ranging from 7 orders of magnitude for the alkaline hydrolysis to 11 orders of magnitude for acid-catalyzed hydrolysis. More recently, Kirby et al.[9,10] reported the rapid hydrolysis in water (under acid conditions) of a highly twisted amide bond in a 1-aza-2-adamantanone, suggesting an even higher acceleration of the hydrolysis rate.

A number of theoretical studies of amide hydrolysis have been made in the gas phase and in solution[4,11−14] and in the presence of explicit water molecules.[15,16] Antonczak et al.[15] found that the presence of a water dimer can induce substantial pyramidalizations in neutral formamide, with the resultant activation of the amide bond. There are also theoretical studies focusing on the structural properties and proton affinities of twisted amides,[17,18] but these contain no characterization of the corresponding transition states and intermediates for hydrolysis. In the present paper, we study the hydrolysis by comparing the activation barrier for a reactant in which the nitrogen is in a pyramidal conformation with that of a planar amide analogue. In line with earlier work on phosphate and sulfate ester hydrolysis, we compare the gas-phase barriers with those in solution to determine how much of the calculated rate acceleration is due to an intrinsic electronic effect (i.e., breakdown of

* Corresponding author. E-mail: marci@tammy.harvard.edu.
[†] Euskal Herriko Unibertsitatea.
[‡] The University of Sheffield.
[§] Université Louis Pasteur.
[||] Harvard University.

10.1021/jp022014s CCC: $25.00
Published on Web 03/12/2003

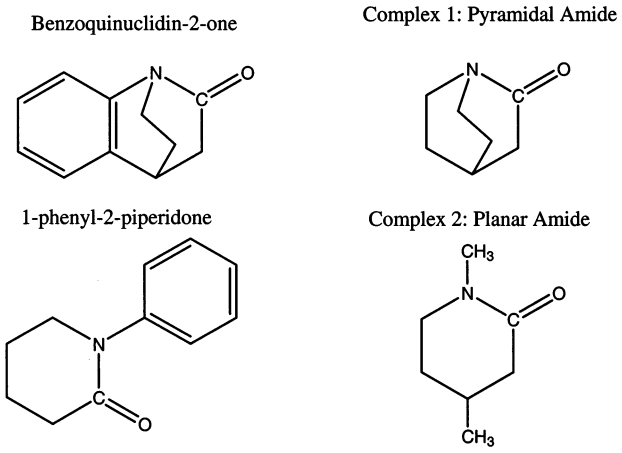

Figure 1. On the left-hand side, amide reactants used by Blackburn et al.[7] to study the rate acceleration for the hydrolysis of amides caused by the C−N bond twist with nitrogen pyramidalization in the reactant. On the right-hand side, our models for the compounds studied experimentally. Notice that complex 2 is the species that results from the hydrogenation of one of the C−C bonds of complex 1. We will call complex 1 the pyramidal or twisted amide throughout the text and complex 2 the unconstrained or planar amide.

the π resonance) and how much to differential solvation of the species involved. We use high-level ab initio calculations to calculate the potential energy surface for the alkaline hydrolysis of a pyramidal amide (complex 1 of Figure 1). This corresponds to a simplified model of the benzoquinuclidin-2-one studied by Blackburn et al.[7] Theoretical calculations have shown[17,18] a high degree of C−N bond twist for that compound in its ground state. We also studied the alkaline hydrolysis for its planar amide analogue (complex 2 of Figure 1), which is obtained by the hydrogenation of one of the C−C bonds of the pyramidal complex. The effect of solvent is introduced by the use of continuum models. Three different solvent models were employed: Poisson−Boltzmann calculations using the UHBD program[19] (PB-U), Poisson−Boltzmann calculations using the Jaguar program[20] (PB-J), and polarizable continuum method (PCM) calculations using the Gaussian 98 suite of programs.[21]

The methods used are described in section 2, and the results are given in section 3. Section 4 presents a concluding discussion.

2. Methodology

Ab initio studies of the potential energy surface for the alkaline hydrolysis of a pyramidal amide (complex 1 of Figure 1) and a planar amide (complex 2 of Figure 1) were made in the gas phase and in solution. All structures were optimized at the B3LYP/6-31+G(d) levels of theory. The out-of-plane deformations are described by the angles τ, χ_C, and χ_N following the definitions of references.[22,23] The angle τ characterizes the mean twisting angle around the C−N bond and ranges from 0° (planar amide group) to 90° (when the two planes defined by the $O_1-C_1-C_2$ and C_5-N-C_6 atoms are perpendicular); χ_C and χ_N are measures of the degree of pyramidalization at the C and N, respectively. They range approximately from 0° (planar sp^2 atoms) to 60° (tetrahedral sp^3 atoms). The combination of dihedrals used to define τ and χ_C and χ_N is as follows. Defining the four torsion angles $\omega_1 = O_1-C_1-N-C_5$, $\omega_2 = C_2-C_1-N-C_6$, $\omega_3 = C_2-C_1-N-C_5$, and $\omega_4 = O_1-C_1-N-C_6$, we can write

$$\tau = \frac{(\omega_1 + \omega_2)}{2} \quad (1)$$

$$\chi_C = \omega_1 - \omega_3 + \pi(mod2\pi) = -\omega_2 + \omega_4 + \pi(mod2\pi) \quad (2)$$

$$\chi_N = \omega_2 - \omega_3 + \pi(mod2\pi) = -\omega_1 + \omega_4 + \pi(mod2\pi) \quad (3)$$

The absolute values for these angles with projection on the 0−90° quadrant are found in Table 1. In all cases, the oxygen atom used to calculate the ω_1 and ω_4 torsion angles corresponds to the original carbonyl oxygen rather than the hydroxide oxygen. For the product structures in which the amide bond is broken, these angles are of limited value. In those cases, we use the improper dihedrals, also indicated in Table 1.

The energies of various species were evaluated at the B3LYP/6-31+G* geometries by single-point calculations at the B3LYP/6-311++G(d,p) level of theory. The use of the B3LYP functional[24−27] is motivated by its success in the evaluation of reliable reaction enthalphies for the hydrolysis of neutral amides.[28] However, in some cases differences are found between B3LYP and other correlated methods such as MP2.[29] To verify that the main conclusions of the paper would not differ by applying another level of theory, single-point MP2 calculations were carried out. The results showed similar qualitative trends to the ones specified throughout the paper.

For determining the enthalpic and entropic corrections,[30] the B3LYP/6-31+G(d) gas-phase frequencies were calculated at the B3LYP/6-31+G(d) geometries. These frequencies were also used to determine the nature of the stationary points encountered. Thus, reactant, intermediate, and product structures showed real frequencies for all of the modes of vibration, whereas TS1 and TS2 structures showed one imaginary frequency along the desired normal mode. The free energy was obtained as a sum of the B3LYP/6-311++G(d,p) energy and the zero-point vibrational energy (ZPVE), the vibrational correction to the ZPVE at 298 K, and the rotational and translational energies at 298 K. The zero-point vibrational energy and the thermal vibrational energy were calculated in the rigid rotor−harmonic oscillator approximation. The rotational and translational energies were treated classically as $^1/_2RT$ per degree of freedom. The calculations were performed using the Gaussian 98 program.[21]

Solvation free energies at the gas-phase B3LYP/6-31+G* geometries were estimated by three methods. They are Poisson−Boltzmann calculations using the UHBD program[19] (PB-U) with the B3LYP/6-31+G(d) Mulliken charges and the standard van der Waals radii for the atoms, Poisson−Boltzmann calculations using the Jaguar program[20] (PB-J), and polarizable continuum method (PCM) using the Gaussian 98 suite of programs.[21] Both PB-J and PCM are self-consistent reaction field (SCRF) methods. In the Poisson−Boltzmann calculations made by Jaguar, the gas-phase wave function is calculated and from that the electrostatic potential. Then a set of atomic charges that fits this electrostatic potential are calculated, and these charges are passed to the Jaguar Poisson−Boltzmann solver, which then determines the reaction field by numerical solution of the Poisson−Boltzmann equations and represents it by a layer of charges at the molecular surface (dielectric continuum boundary). These "solvent" point charges are returned to the SCF program, which performs another quantum mechanical wave function calculation, which incorporates the solvent charges. This process is repeated until self-consistency is achieved. In the polarizable continuum method (PCM),[27,31,32] the solute molecule is embedded in a cavity in a dielectric medium that represents the solvent. Solute−solvent interactions are described

TABLE 1: B3LYP/6-31+G* Geometrical Parameters for the Stationary Points of the PESs of the Hydrolysis of Twisted/Pyramidal and Planar Amides[a]

	bond distances						angles			improper dh.	
molecule	C_1N	C_1O_1	C_1O_2	O_1H	O_2H	NH	τ	χ_C	χ_N	N	C_1
formamide	1.361	1.219					0.1	0.1	0.1	180.0	180.0
formamide (TS)	1.439	1.203					90.0	0.1	64.8	115.2	179.9
pyramidal											
React	1.453	1.209					89.4	0.1	62.4	117.3	179.8
$TS1_{py}$	1.466	1.220	2.667		0.971	3.648	69.5	17.6	61.8	120.1	162.4
INT_{py}	1.554	1.227	1.493		0.972	2.764	53.5	52.7	60.0	119.0	127.3
$TS2_{py}$	2.378	1.226	1.400		0.994	1.894	41.5	56.1	66.0	115.9	162.8
$PROD_{py}$	3.375	1.257	1.270	2.008		1.026	42.4	60.1	70.6	115.9	179.1
planar											
React	1.375	1.232					3.1	2.9	11.6	169.5	177.2
$TS1_{chair}$	1.408	1.243	2.308		0.971	3.199	5.9	24.9	44.3	137.2	155.1
$INT1_{chair}$	1.516	1.298	1.548		0.971	2.973	3.8	52.2	50.7	130.5	127.4
$INT2_{chair}$	1.542	1.495	1.310	0.972	2.130	2.982	0.4	70.4	57.8	122.0	128.9
$INT3_{chair}$	1.570	1.509	1.287	0.973		2.340	3.3	70.5	60.0	120.4	129.1
$TS2_{chair}$	2.341	1.393	1.228	0.996		1.883	19.4	66.7	55.6	127.4	156.0
$PROD_{chair}$	3.394	1.274	1.255	1.871		1.029	32.6	60.3	29.0	127.8	178.7
$TS1_{boat}$	1.419	1.248	2.156		0.971	3.170	12.2	29.2	41.9	139.3	150.8
INT_{boat}	1.511	1.292	1.553		0.971	2.985	14.2	52.0	48.0	132.9	128.0

[a] Distances are in angstroms, and angles are in degrees.

by a reaction potential arising from the presence of the dielectric medium. The polarization of the solvent is represented by a charge density σ introduced on the surface S of the cavity surrounding the solute, and the corresponding reaction-field potential takes the form

$$\phi(r) = \int_S d^2 r^t \frac{\sigma(r^t)}{|r - r^t|} \quad (4)$$

For both PB-J and PCM, the B3LYP/6-311++G(d,p) level of theory was employed. In the case of the PB-J calculations, the default atomic van der Waals of the Jaguar program were used.[20] In the case of the PCM calculations with Gaussian 98, the UAHF (united atom Hartree−Fock) parametrization[33] of the polarizable continuum model was used. All of these solvation calculations were made at the gas-phase B3LYP/6-31+G* geometries, and we consider this to be the main limitation of this paper. Preliminary attempts to optimize the transition states in solution using PCM models led to problems in the convergence, which are associated with discontinuities in the solvation potential.[34] However, according to the agreement between our data and experiments for the differential in barriers between the two reactions (see Discussion section), the lack of geometry optimization does not seem to introduce major errors when estimating the rate acceleration of a pyramidal amide with respect to that of the planar amide. Probably this is an indication that geometry optimization in solution will have a similar effect for both reactions, and they tend to cancel when comparing relative energy barriers.

3. Results

3.1. Gas Phase. 3.1.1. Twisted Amide Reactant. Structures. The stationary points for the hydrolysis of the twisted (pyramidal) amide are shown in Figure 2. Structural and energetic data are given in Tables 1 and 2, respectively. Figure 2 shows that the reaction goes through an intermediate, so that there are five stationary points: $React_{py}$, $TS1_{py}$, INT_{py}, $TS2_{py}$, and $PROD_{py}$. The pyramidalization of the nitrogen and the twist of the amide bond are measured by the values of the χ_N and τ angles, respectively. Values obtained for these angles in formamide are also included for comparison. In a standard amide bond, such as the one found in formamide, the amidic group is planar, which corresponds to a "nontwist" situation (τ is 0°), and both carbon and nitrogen show planar sp^2 hybridization (the corresponding χ angles are 0°). In the twisted amide reactant, we find that the nitrogen is significantly pyramidalized, with a χ_N value of 62.4°, and that the peptide bond is substantially twisted, with a τ angle of 89.4°. A similar twist has been reported[18] for this compound at the HF/6-31G* level of theory. The planarity of the carbonyl group is kept at values similar to the ones found in formamide (χ_C is 0.1°). The values of the bond distances for the peptide bond reflect this twist of the amide bond and the pyramidalization of the nitrogen. The amide (C_1−N) bond length is 1.453 Å, almost 0.1 Å longer than in formamide, whereas the C_1═O_1 distance is 1.209 Å, very close to the 1.219 Å found in formamide. These distances are slightly longer than the bond distances reported by Greenberg et al.;[18] namely, they obtained a C−N distance of 1.433 Å and a C−O distance of 1.183 Å. The slight elongation is a consequence of the fact that the present calculations include electron correlation, which tends to elongate bonds. The significant elongation of the C−N bond and the relative small shrinking of the C−O bond in the twisted amide follow the trend observed when rotating the amide bond in formamide and its derivatives.[35−40] This fact, along with the small charge transfer to oxygen with the twist of the amide bond, has motivated a revision of the traditional amide resonance model.[37,40−42] The apparent contradiction with the amide resonance model can be reconciled if one takes into account the strong polarization of the C═O bond and its ionic bond character.[40] In fact, Glendenning et al.[42] has determined the role and extent of resonance interactions in formamide by using the natural population analysis[43] and natural resonance theory.[44] They found that the NRT representation of planar amides consists primarily of two resonant structures, which include strong delocalizations of the $n_N \rightarrow \pi^*_{CO}$ type, in agreement with traditional amide model.

Next, we analyze the structures for the TSs, intermediates, and products of the hydroxide attack. In terms of the τ and χ angles, there are two aspects of interest. The χ_N angle shows little change upon hydroxide attack (i.e., the pyramidalization at the nitrogen is not affected by the hydroxide attack). In contrast, the χ_C angle increases from 0.1° to close to 60°,

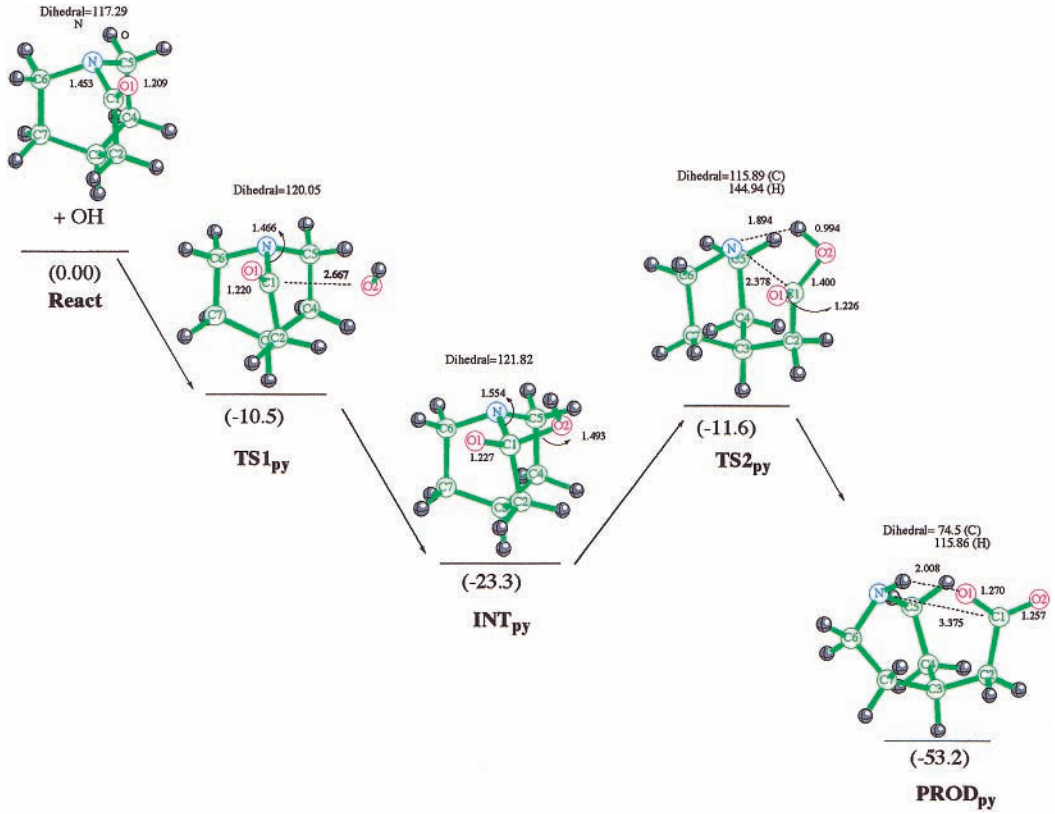

Figure 2. B3LYP/6-31+G(d) structures in the hydrolysis of the twisted/pyramidal amide. Numbers in parentheses correspond to ΔG_{gas} values. Energies are in kcal/mol relative to the energies of the reactants.

TABLE 2: Ab Initio Energies and Free Energies in the Gas Phase and in Solution at B3LYP/6-311++G(d,p) for the Hydrolysis of Twisted/Pyramidal and Planar Amides[a]

	gas phase		solvation free energy			solution phase		
molecule	ΔE	ΔG_{gas}	G_s^{PB-U}	G_s^{PB-J}	G_s^{PCM}	ΔG_{aq}^{PB-U}	ΔG_{aq}^{PB-J}	ΔG_{aq}^{PCM}
OH^-			−95.1	−105.5	−109.8			
				pyramidal amide				
React	0.0	0.0	−9.6	−11.5	−9.8	0.0	0.0	0.0
$TS1_{py}$	−20.8	−10.5	−73.6	−78.1	−71.6	20.6	28.4	37.5
INT_{py}	−36.2	−23.3	−73.7	−73.6	−72.6	7.7	20.1	23.7
$TS2_{py}$	−21.8	−11.6	−71.2	−60.5	−57.0	21.9	44.9	51.0
$PROD_{py}$	−65.5	−53.2	−66.8	−71.0	−73.2	−15.3	−7.2	−6.8
				planar amide				
React	0.0	0.0	−7.4	−10.9	−8.0	0.0	0.0	0.0
$TS1_{chair}$	−16.4	−5.6	−66.8	−76.1	−67.7	30.1	34.7	44.5
$INT1_{chair}$	−19.7	−7.6	−67.9	−62.3	−69.8	27.0	46.5	40.5
$INT2_{chair}$	−19.2	−6.9	−67.6	−73.4	−79.8	28.0	36.1	31.2
$INT3_{chair}$	−15.0	−3.1	−69.1	−77.7	−74.0	30.3	35.6	40.7
$TS2_{chair}$	−4.7	5.1	−60.3	−58.1	−57.2	47.3	63.4	65.7
$PROD_{chair}$	−40.8	−30.7	−62.6	−66.7	−71.1	9.2	19.0	16.0
$TS1_{boat}$	−12.9	−2.3	−67.0	−76.4	−68.3	33.2	37.7	47.2
INT_{boat}	−15.5	−4.1	−67.6	−67.0	−71.8	30.8	45.3	41.9

[a] Three approximations were used for the estimation of relative free energies in solution: Poisson−Boltzmann (PB) calculations using B3LYP/6-31+G* Mulliken charges and the UHBD program,[19] Poisson−Boltzmann calculations using the Jaguar program[20] (PB-J) and the B3LYP/6-311++G(d,p) electron density, and PCM calculations (PCM) with the B3LYP/6-311++G(d,p) method and Gaussian 98 program.[21] The corresponding solvation free energies (G_s) are also shown. All quantitaties are in kcal/mol. Experimental values[46,47] for the solvation free energy of OH^- range from −104.0 to −107.5 kcal/mol.

indicative of the loss of planarity at the carbonyl carbon as the nucleophilic attack takes place. The change in C hybridization also causes τ to decrease.

The transition state for the attack of the hydroxide anion ($TS1_{py}$) is early, with a $C_1-O_2(H)$ distance of 2.67 Å relative to the value (1.49 Å) in the intermediate. The other geometrical parameters are only slightly altered with respect to their values in the amide reactant (see Table 1) (e.g., the carbonyl bond distance is 1.220 Å, and the amide bond distance is 1.466 Å, both very close to their original values). After hydroxide attack, an intermediate INT_{py} is formed; it is the so-called "tetrahedral intermediate" of the amide hydrolysis reaction. The C_1-O_2H distance is 1.493 Å, and the amide bond is significantly elongated (1.554 Å) with respect to that of the reactant. The crystal structure of a similar compound (1-aza-2-adamantanone) reported by Kirby et al.[10] gives a value of 1.552 Å for the amide bond in the intermediate, in very good agreement with our theoretical estimates. However, they report a C−O distance of

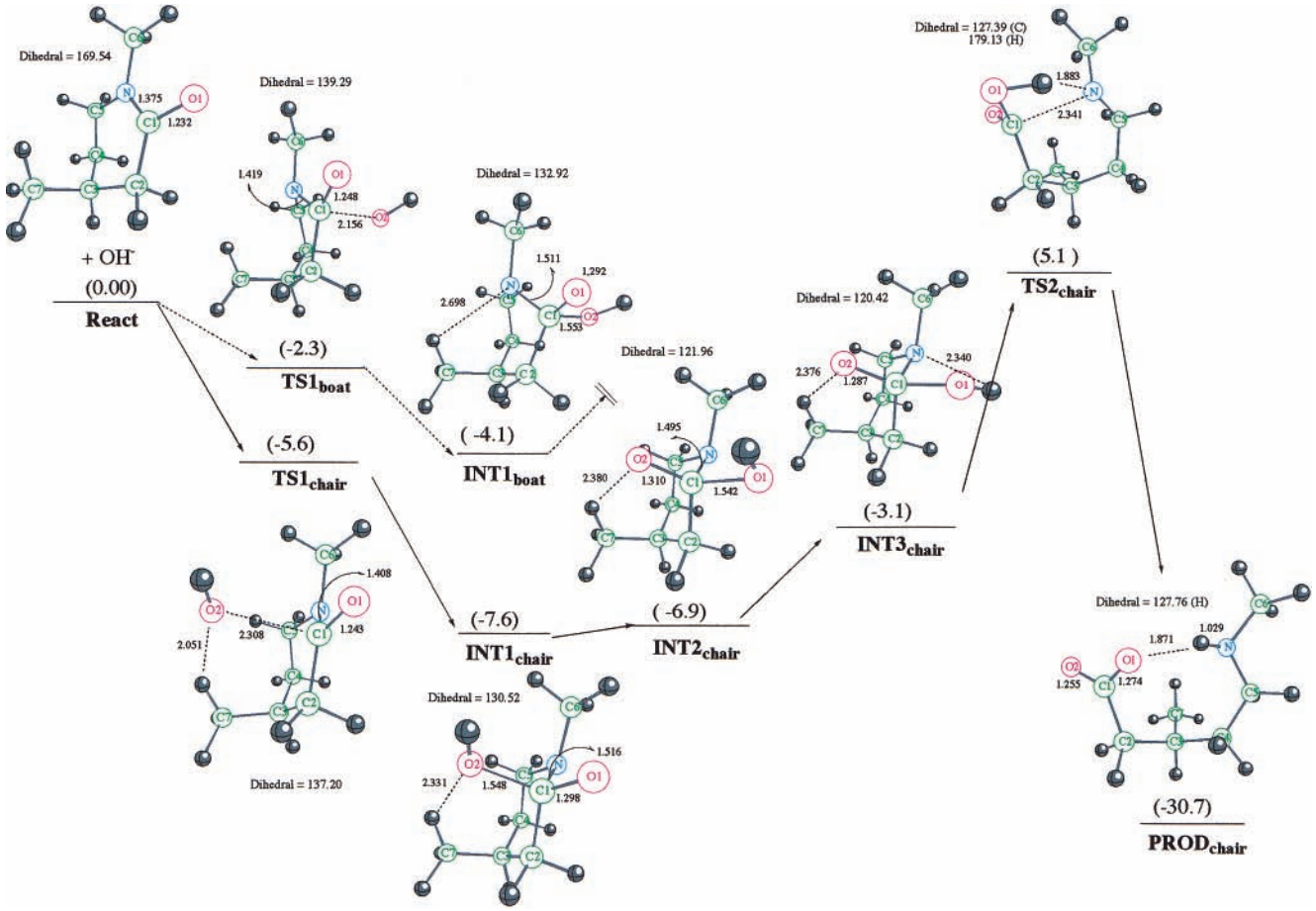

Figure 3. B3LYP/6-31+G(d) structures in the hydrolysis of the planar amide. Numbers in parentheses correspond to ΔG_{gas} values. Energies are in kcal/mol relative to the energies of the reactants.

1.382 Å, which is between our 1.227 Å for C_1-O_1 and 1.493 Å for C_1-O_2. The apparent discrepancy between the theoretical and crystallographic C−O bond distances is due to the different protonation states of the oxygens in the crystal structure and in our structure. At the pH at which the crystal structure was determined (0.1 M HCl, i.e., pH around 1), both oxygens are protonated rather than only one of them, as in our case. When the same protonation state is considered, we obtain a value of 1.389 Å at B3LYP/6-31+G*, indicating that our level of theory is satisfactory for the geometries of these compounds. The χ_C angle now is very close to 60°, namely, 52.7°, and it reflects the expected trend of the transition between an sp^2 and an sp^3 carbon as the hydroxide attack takes place. The next step of the reaction corresponds to breaking the C_1-N amide bond, which is concerted with proton transfer from the nascent carboxylic acid group to the departing nitrogen. The transition state for this second step is $TS2_{py}$. At the transition state, the proton is oriented toward the nitrogen, and their separation is only 1.894 Å. The $C_1-O_2(H)$ bond distance has decreased to 1.400 Å, and the amide C−N distance has increased to 2.378 Å. Since the peptide bond is being broken, τ loses its meaning, and the χ angles are of limited value for describing the planarity of the C and N atoms. For these structures, it is better to look at the improper dihedrals for these atoms. (See Table 1.) After the complete breaking of the amide bond and the transfer of the proton to the nitrogen, the product structure $PROD_{py}$ is obtained. In this structure, the carboxylate is anionic, with a C_1-N distance of 3.375 Å. Carbon has recovered its planarity according to the value of the $C_2-C_1-O_1-O_2$ dihedral angle of 179.1°. The structure is stabilized by an intramolecular hydrogen bond between the NH proton and one of the carboxylate oxygens. This hydrogen bond slightly enhances the pyramidalization of the nitrogen; the value defined in terms of the $H-N-C_5-C_6$ dihedral angle is 115.9°.

Energy Profile. The energies (relative to those of the reactants) of the stationary points described above are in Table 2 and in Figure 6. All stationary points show a lower energy than the reactants, even when entropic and enthalpic corrections are included. The transition state for the hydroxide attack, $TS1_{py}$, has a ΔG_{gas} of −10.5 kcal/mol. This negative ΔG_{gas} for the transition state is indicative of the existence of the expected ion−molecule complex for the approach of the hydroxide to the amide. These ion−molecule complexes are characteristic of the gas-phase reaction, but they will no longer be stable species in aqueous media. To demonstrate this, we have trapped an ion−molecule complex in the potential energy surfaces. Its geometry can be found in Figure 4. The ion−molecule complex forms a hydrogen bond with an aliphatic C−H bond of the cage. Its ΔG_{gas} is −16.9 kcal/mol. However, after solvation corrections are introduced using the PCM model, its energy is 34.7 kcal/mol, indicating that it will not be a stable species in solution.

The intermediate INT_{py} formed after the hydroxide attack is very stable (i.e., ΔG_{gas} of −23.3 kcal/mol). The barrier for the breaking of the C−N bond in this intermediate is 11.7 kcal/mol, the $TS2_{py}$ transition state having a slightly lower ΔG_{gas} than the $TS1_{py}$ transition state. The breaking of the amide bond is concerted with a transfer of a proton to the nitrogen from the carboxyl group (Figure 2) and makes the resultant product $PROD_{py}$ very stable; ΔG_{gas} is −53.2 kcal/mol. Thus, $PROD_{py}$ is the global minimum along this potential energy surface and

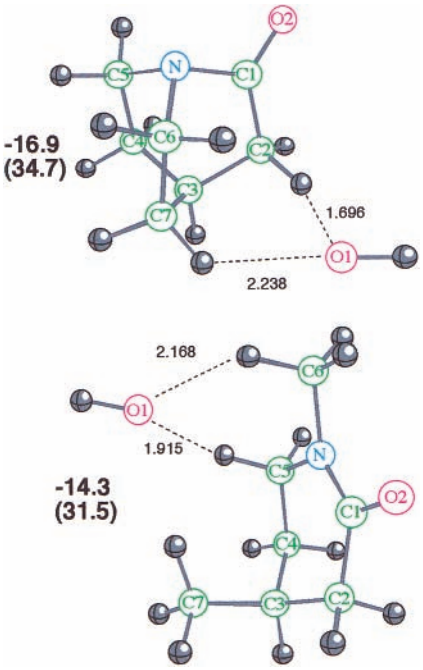

Figure 4. B3LYP/6-31+G(d) structures for ion−molecule complexes in the gas phase. These complexes are formed from the reactants without a barrier. Bold numbers correspond to ΔG_{gas} and ΔG_{aq}^{PCM} (in parentheses) values. Energies are in kcal/mol relative to the energies of the reactants. In solution, these complexes are not stable.

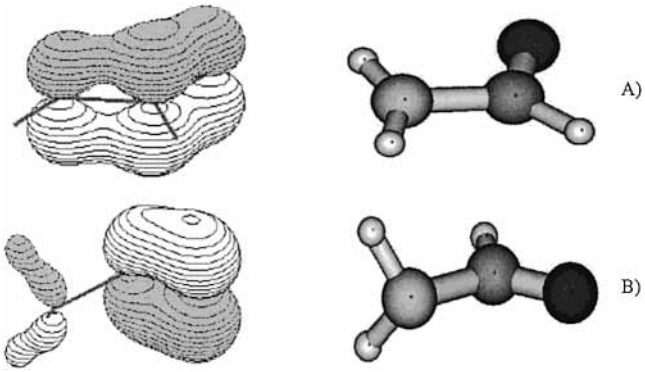

Figure 5. Formamide, ground-state geometry (A), and transition-state geometry corresponding to the rotation along the C−N bond with the loss of the $n_N \rightarrow \pi^*_{CO}$ resonance. Notice the planar N conformation in A and the pyramidal conformation in B. On the left is the HOMO-3 orbital, indicating the π resonance along N−C−O linkage for the planar case.

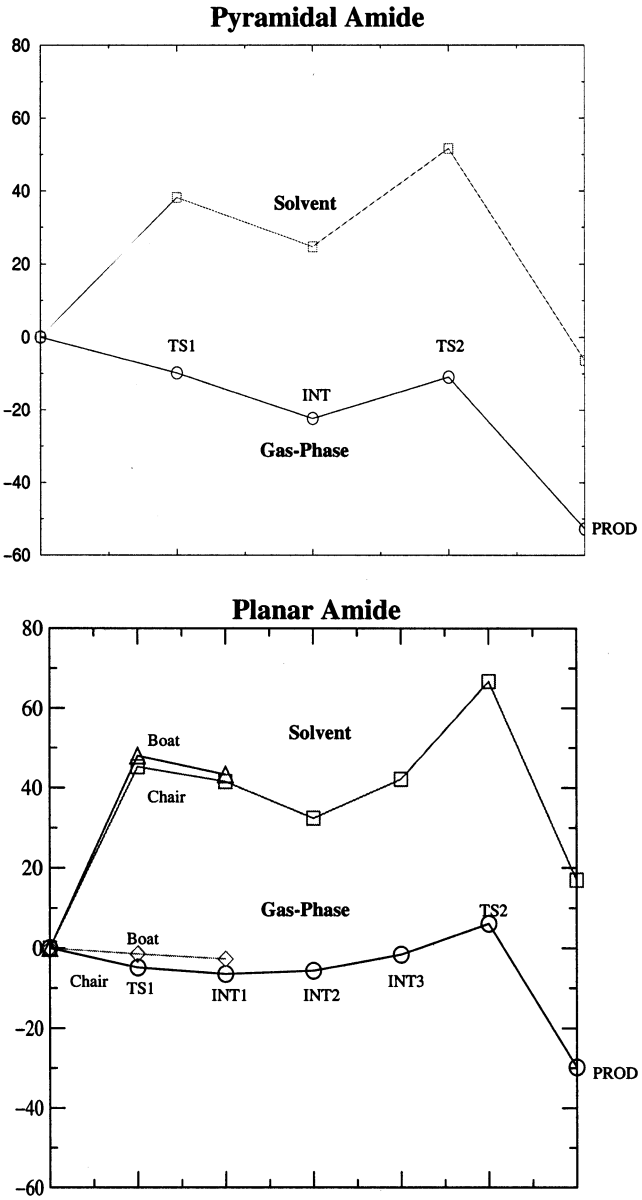

Figure 6. Diagram showing the relative energies (kcal/mol) with respect to the reactants for the hydrolysis of the twisted/pyramidal amide (top diagram) and for the hydrolysis of the planar amide (bottom diagram). Both the gas-phase profile and the solvated profile are shown (estimated using the PCM results of Table 2). In the planar case, two possible conformations for the hydroxide attack were considered for the first step of the reaction: boat and chair conformations. Both are included in the diagram. See the text for further explanations.

has a lower energy than INT_{py}. This is a consequence of the fact that the O_1 oxygen in INT_{py} can form only a single bond with C_1 because this carbon is already involved in three other bonds (C_1-O_2, C_1-C_2, and C_1-N). However, in $PROD_{py}$, the C_1-N bond is broken, and O_1 forms a double bond with C_1. In addition, since the proton at O_2 has been transferred to the nitrogen, there is considerable resonance stabilization of the π electrons in the $\pi_{O_1-C-O_2}$ delocalized orbital.

3.1.2. Planar Amide Reactant. Structures. The B3LYP/6-31+G* optimized structures for the reaction are shown in Figure 3. As can be seen, the potential energy surface for the planar amide reaction is more complicated than for the constrained pyramidal amide. This is due to the greater flexibility of the monocyclic lactam ring compared with that of the more rigid bicyclic lactam structure. There are two possible initial transition states, $TS1_{chair}$ and $TS1_{boat}$. These lead, respectively, to chair and boat intermediates. There are three chair ($INT1_{chair}$, $INT2_{chair}$, and $INT3_{chair}$) intermediates and one boat intermediate (INT_{boat}) that are stable (local minima) species. We also characterized a transition state for the breaking of the C_1-N bond, $TS2_{chair}$, and the final product of the reaction, $PROD_{chair}$. Boat structures beyond INT_{boat} were not considered because of the higher energy of these structures as compared with that of the chair conformers. The flexibility of the monocyclic lactam ring will presumably makes possible other intermediates of similar energy to the ones we have shown. Besides, transition states interconnecting intermediates were not determined. This is justified in the context of the present paper because our main focus is to compare the energetics of the transition states corresponding to the formation of the tetrahedral intermediate (TS1) and the breakdown of the C−N bond (TS2) for the hydrolysis of a twisted amide and its planar counterpart. The difference in the

barriers for these two TSs determines the relative reaction rates for the two reactions.

The planar amide reactant is a six-membered lactam ring. The value of τ, 3.1°, indicates that there is almost no twist in the peptide bond, and the low value of χ_N, 11.6°, describes a nearly planar nitrogen atom. Thus, the $n_N \rightarrow \pi^*_{CO}$ resonance is presumably very similar to the one in formamide, which makes this compound a good model system for comparison with the hydrolysis of the pyramidal amide. The deviation from planarity in χ_N arises from a tendency toward a chair conformation to avoid eclipsing the methylene hydrogens; it contributes to a partial loss of the $n_N \rightarrow \pi^*_{CO}$ resonance. On the basis of the values of the amide bond distances, we expect this loss to be small since the amide bond distance is only 0.014 Å larger than the one in formamide. As the reaction proceeds and the intermediate is formed, the value of χ_C increases to 60°, similar to what was calculated in the hydrolysis of the twisted amide. Contrary to the twisted amide case, χ_N changes substantially as the hydroxide approaches (i.e., the nitrogen goes from being almost planar in the reactant to being pyramidal in the intermediates). Consequently, χ_N increases from a value of 11.6° in the reactant to a value of 50−60° in the intermediates.

The two transition states for the attack of the hydroxide ion on the carbonyl carbon, $TS1_{chair}$ and $TS1_{boat}$, differ as to the side of the ring on which the attack takes place. $TS1_{chair}$ involves the attack of the OH^- on the side of the C_3-methyl group, and $TS1_{boat}$ corresponds to the attack on the opposite side. (See Figure 3.) The large repulsion between the nitrogen lone pair and the incoming hydroxide anion leads to an accentuation of the chair conformation of the ring in the former and to the boat conformation in the latter. In the constrained system (see Figure 2), only the boat conformation is possible. Interestingly, the $C_1-O_2(H)$ distance in $TS1_{chair}$ is significantly longer (2.308 Å) than in $TS1_{boat}$ (2.156 Å). In both TSs, the nitrogen has attained a significant degree of pyramidalization according to both the χ_N angle and the improper dihedral. Thus, χ_N has been augmented from 11.6° in the reactant to 44.3° in $TS1_{chair}$ and 41.9° in $TS1_{boat}$ (i.e., χ_N has been augmented by 30−33°). If pyramidalization is measured according to the decrease in the $C_1-N-C_5-C_6$ pseudodihedral angle (from 180° for planar nitrogen to 120° for pyramidal nitrogen), then a similar change of 30° is observed. Therefore, a substantial decrease in the $n_N \rightarrow \pi^*_{CO}$ resonance in these structures is expected. (See section 4.)

A boat intermediate, INT_{boat}, and three chair structures, $INT1_{chair}$, $INT2_{chair}$, and $INT3_{chair}$, are shown in Figure 3. All of the vibrational frequencies characterized for these stationary points were real (i.e., positive force constants), demonstrating that they are stable minima of the potential energy surface. There is considerable pyramidalization of the nitrogen in all of the intermediates (see Table 1), evidenced by both χ_N and the $C_1-N-C_5-C_6$ pseudodihedral angle. The C_1-N amide bond length in the intermediates varies significantly depending on the orientation of the proton of the $>CO_2H$ group. For the three chair conformations, the shortest C_1-N bond length is obtained for $INT1_{chair}$ (1.516 Å), the structure with the proton on the oxygen furthest from nitrogen. When the proton is transferred to the other oxygen of the carboxyl group ($INT2_{chair}$), the C_1-N distance is elongated to 1.542 Å, and when the proton is oriented toward the nitrogen in $INT3_{chair}$, the distance is 1.570 Å.

For the second step of the reaction, which involves the breaking of the amide C−N bond, we have analyzed only the chair pathway. The reaction from boat conformers is expected to lead to a higher-energy transition state since boat conformers were higher in energy for TS1 and INT1. (See the Energy Profile section below.) However, the boat conformer could be converted to the chair conformer by an inversion at the nitrogen, which is not studied in the present work. The transition state, $TS2_{chair}$, for the breaking of the C_1-N amide bond is concerted with O-to-N proton transfer. The $TS2_{chair}$ transition state connects the $INT3_{chair}$ intermediate with the $PROD_{chair}$ structure. The C_1-N and N−H distances are very similar to those found for $TS2_{py}$. (See Table 1.) $PROD_{chair}$ is formed by breaking the C_1-N bond. An intramolecular hydrogen bond is formed between the H(N) and the carboxyl group, and the geometrical parameters are again similar to the pyramidal case. The shorter $O_1-H(N)$ hydrogen bond distance (1.871 Å) is possible because of the greater flexibility of this structure, as compared with that of the $PROD_{py}$ product.

Energy Profile. The values of ΔG_{gas} for all of the stationary points on the unconstrained amide are larger than the corresponding values for the hydrolysis of the pyramidal amide. (See Table 2.) This is due to the energy required for pyramidalization of the nitrogen along the reaction path of the planar system, in contrast to the constrained amide that is already destabilized by the pyramidalization of its nitrogen. This point is considered in more detail in the Discussion section. The reaction is qualitatively similar to that of the pyramidal case in that ion−molecule complexes form as the first step of the reaction in the gas phase and the transition states for the hydroxide attack and formation of the tetrahedral intermediates are lower in energy than the reactants (i.e., ΔG_{gas} is −2.3 kcal/mol for $TS1_{boat}$ and −5.6 for $TS1_{chair}$). As in the pyramidal case, we have characterized one of the possible ion−molecule complexes (Figure 4), which showed a ΔG_{gas} of −14.3 kcal/mol. After solvent corrections are included, the ΔG^{PCM}_{aq} is 31.5 kcal/mol; therefore, this kind of stationary point in the gas phase is not going to be relevant to the reaction in solution, and we focus on the rest of the stationary points throughout the paper.

The four intermediate structures have free energies between −7.6 and −3.1 kcal/mol, substantially larger than the −22.3 kcal/mol value obtained for the intermediate, INT_{py}, of the pyramidal system. The differences in energy among the four intermediates are related to two factors: the chair−boat conformation and the orientation of the carboxylic proton. From the relative energies for $INT1_{chair}$ and INT_{boat}, we estimate a value of 4.0 kcal/mol for the boat versus chair stabilization. By comparing $INT2_{chair}$ and $INT3_{chair}$, we see that there is also a 4.0 kcal/mol energy penalty for a change in the orientation of the carboxylic proton from a position in which it is oriented toward one of the lone pairs of the other carboxylic ($INT2_{chair}$) oxygen to one where it is oriented toward the lone pair of the nitrogen ($INT3_{chair}$). However, it is only from the latter (less stable) structure that the proton can be transferred to the nitrogen in $TS2_{chair}$.

The transition state for the breaking of the C_1-N amide bond is 5.1 kcal/mol with respect to the reactants, and it is the stationary point of highest energy on the potential energy surface. The barrier with respect to $INT3_{chair}$ is 8.0 kcal/mol, almost 4.0 kcal/mol lower than in the pyramidal case. This is attributable to the 4.0 kcal/mol destabilization of $INT3_{chair}$ in orienting the proton toward the nitrogen (see above).

The product structure $PROD_{chair}$ is formed by breaking the C_1-N bond. It is the most stable structure on the potential energy surface, namely, −30.7 kcal/mol relative to the reactants. However, this relative stability is significantly less than that for the product $PROD_{py}$ (−52.7 kcal/mol). As we discuss in section 4, this difference is due to the destabilization of the pyramidal amide reactant by the loss of $n_N \rightarrow \pi^*_{CO}$ resonance.

3.2. Hydrolysis in Solution. Solvation free energies and the relative free energies in solution for each of the compounds are shown in Table 2. The gas-phase and solution reaction free-energy profiles are presented in Figure 6.

The three methods used to evaluate the solvent free energies (Poisson−Boltzmann with UHBD (PB-U), Poisson−Boltzmann with Jaguar (PB-J) and PCM) give qualitatively similar solvent effects for the reaction. Solvation favors the separate reactants over the transition states and intermediates so that the solvent increases the barrier to hydrolysis. This corresponds to what has been reported by Weiner et al.[11] for the alkaline hydrolysis of formamide. The better solvation of the hydroxide anion relative to that of the transition state and intermediates, where the negative charge is delocalized over the entire molecule, is the origin of the enhanced barrier. This result is similar to what has been found in other ion−molecule reactions.[45]

However, there are quantitative differences among the three methods for some of the structures. For instance, the solvation free energy of the hydroxide anion is −109.8 kcal/mol at PCM, −105.5 kcal/mol at PB-J, and −95.1 kcal/mol at PB-U. The experimental solvation free energy of the hydroxy anion range from −104.0 to −107.5 kcal/mol.[46,47] Thus, both PB-J and PCM fit the proposed experimental values for OH^-, whereas the value at PB-U is too small. Thus, we consider mainly the PCM and PB-J results in what follows.

3.2.1. Pyramidal Amide Reactant. In contrast to the gas-phase potential energy surfaces, almost all of the relative free energies with respect to the reactants are positive, as can be seen from the solution-phase free energies (ΔG_{aq}^{PCM}) in Table 2; the sole exception is the product free energy, which is still negative, though much less so than in the gas phase. The largest differences in solvation free energies between PB-J and PCM occur for $TS1_{py}$, −78.1 kcal/mol for the former and −71.6 kcal/mol for the latter. As a consequence, the barrier obtained with PB-J for the first step of the reaction (hydroxide addition) is lower than the one obtained with PCM, namely, 28.4 kcal/mol versus 37.5 kcal/mol, respectively. This difference arises mainly from the solvation free energy of OH^- (see above). The agreement between PB-J and PCM solvation free energies is better for other stationary points, especially for the INT_{py} structure. The intermediate is at 20.1/23.7 kcal/mol (PB-J/PCM) with respect to the reactants. Both PB-J and PCM give the lowest solvation free energy for the $TS2_{py}$ structure, −60.5 kcal/mol (PB-J) and −57.0 kcal/mol (PCM). Because of this, $TS2_{py}$ is the stationary point with highest ΔG_{aq}^{PB-J} and ΔG_{aq}^{PCM}, 44.9 and 51.0 kcal/mol, respectively. Finally, the exothermicity of the reaction is maintained with solvation but to a much lower degree than in the gas phase. The reaction is now slightly exothermic by −7.2 kcal/mol at PB-J and −6.8 kcal/mol at PCM.

Although the solvation free energies vary significantly, the barrier for hydroxide attack ($\Delta G_{aq}[TS1_{py}] - \Delta G_{aq}[React]$) is larger than the barrier for the C−N bond breaking ($\Delta G_{aq}[TS2_{py}] - \Delta G_{aq}[INT_{py}]$) for all three methods, as shown in Table 2. The importance of this in the overall reaction is discussed in section 4.4.

3.2.2. Planar Amide Reactant. As in the case of the pyramidal reactant, the planar-system solvation correction leads to more positive relative free energies. In fact, all species, including the product, are less stable than the reactants. The difference between the pyramidal and planar reactant species originates in the gas-phase free energies rather than in the solvation free energies, which are similar. After adding the solvation free energies to ΔG_{gas} (see Table 2), all of the species have values of ΔG_{aq} larger than those obtained in the reaction of the pyramidal amide. Again, the solvation corrections differ significantly depending on the method, but this general behavior is independent of the method. For example, in the lowest-energy chair pathway, the barrier for hydroxide attack is 6.3/7.0 kcal/mol (PB-J/PCM) higher than in the hydrolysis of the pyramidal amide. If we make the comparison with the boat pathway, then this difference increases to 9.3/9.7 kcal/mol. These differential barriers between the hydrolysis of the pyramidal and planar amides are about 4.0 kcal/mol larger than in the gas phase. Thus, solvent favors the hydroxide attack on the pyramidal amide with respect to the planar amide by a nonnegligible factor.

The two transition states for the hydroxide approach ($TS1_{chair}$ and $TS1_{boat}$) have similar solvation free energies, −76.1/−67.7 and −76.4/−68.3 kcal/mol (PB-J/PCM), respectively. They are somewhat smaller in absolute value than the solvation free energy of $TS1_{py}$ (−78.6/−71.6 kcal/mol at PB-J/PCM). However, the solvation free energies calculated with PB-J are 8.0−9.0 kcal/mol larger in absolute value than those calculated with PCM. In contrast to $TS1_{chair}$ and $TS1_{boat}$, the intermediates show a wide range of solvation free energies. Except for $INT3_{chair}$, the PB-J solvation free energies are smaller in absolute value than the PCM ones. PB-J and PCM agree in having $INT1_{chair}$ as the intermediate with the lowest solvation free energy. However, the largest solvation free energy in absolute value is obtained for $INT3_{chair}$ with PB-J and for $INT2_{chair}$ with PCM. The smallest solvation free energy in absolute value is found for $TS2_{chair}$ with both PB-J and PCM levels.

The planar intermediates show positive ΔG_{aq} at PB-J and PCM levels of theory. The relative stabilities change somewhat when the solvent contributions are added. For PB-J,

$$INT3_{chair}\ (35.6) \approx INT2_{chair}\ (36.1) > INT_{boat}\ (45.3) > INT1_{chair}\ (46.5)$$

whereas for PCM

$$INT2_{chair}\ (31.2) > INT1_{chair}\ (40.5) > INT3_{chair}\ (40.7) > INT_{boat}\ (41.9)$$

where the numbers in parentheses correspond to the ΔG_{aq} for each of the isomers in kcal/mol.

Both PB-J and PCM solvent contributions stabilize the $INT2_{chair}$ intermediate with respect to the other intermediates. However, the solvent stabilization of $INT3_{chair}$ observed with PB-J is less clear since the same is not obtained with PCM. By contrast, there is destabilization of the $INT1_{chair}$ structure. This is the most stable intermediate in the gas phase, but it is the least stable at PB-J (46.5 kcal/mol) and is 9.3 kcal/mol larger in energy than $INT2_{chair}$ at PCM. The ΔG_{aq}^{PB-J} value for $INT1_{chair}$ is 12.0 kcal/mol larger that the ΔG_{aq}^{PB-J} of $TS1_{chair}$. This indicates that the solvent could significantly distort the transition state in solution to geometries closer to $INT1_{chair}$ by reducing the $C_1-O_2(H)$ bond length.

The ΔG_{aq} for $TS2_{chair}$ is similar to the values of PB-J (63.4 kcal/mol) and PCM (65.7 kcal/mol). The barrier for the breaking of the amide bond, calculated with respect to $INT3_{chair}$, is 27.8/25.0 kcal/mol (PB-J/PCM), which is substantially larger than the 8.0 kcal/mol gas-phase barrier. The cause of this barrier enhancement is mainly the small solvation free energy for structure $TS2_{chair}$ relative to that of the intermediate. The barrier is only 3.0 kcal/mol lower than the barrier of the pyramidal complex. $PROD_{chair}$ is significantly destabilized by the solvent,

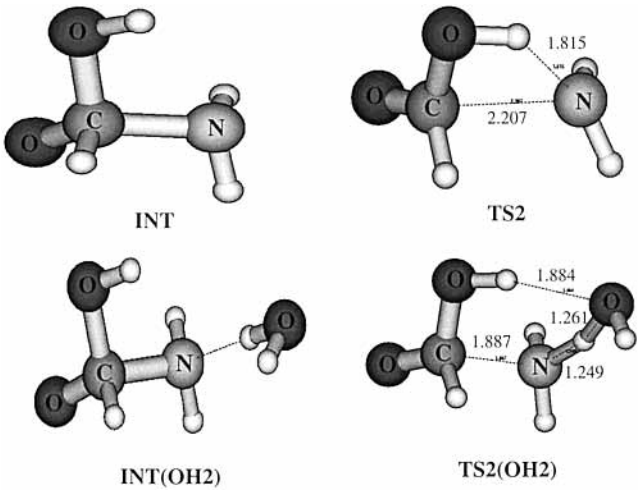

Figure 7. Intermediate and TS2 transition-state structures in the hydrolysis of formamide characterized at the B3LYP/6-31++G(d,p) level of theory.

and the reaction is now endothermic by 19.0/16.0 kcal/mol at PB-J/PCM levels of theory.

3.3. Water-Assisted Breakdown of the Tetrahedral Intermediate. The breakdown of the tetrahedral intermediate (INT_{py} and $INT3_{chair}$ in Figures 2 and 3, respectively) involves the transition states of largest energy with respect to the reactants, as shown in Figure 6. Both $TS2_{py}$ and $TS2_{chair}$ structures correspond to the cleavage of the C−N bond concerted with a proton transfer from the carboxylic acid to nitrogen. The transition states resemble a four-membered ring in which all the bonds that are breaking and forming are part of the ring. In the case of formamide, it has been reported[11,15,48] that an explicit water molecule from the solvent can assist in this proton transfer. This water molecule acts as a proton bridge between one of the carboxylic oxygens and nitrogen, receiving the proton of the oxygen and donating, in turn, one of its protons to nitrogen. The resultant transition state has a six-membered ring structure (see Figure 7). Explicit water molecules have also been found to have a substantial effect on the one-step concerted mechanism of the hydrolysis of neutral formamide. Antonczak et al.[15] found that the hydrogen bond interaction between a water dimer and formamide led to substantial pyramidalization of the nitrogen in the reagents because of the high proton-donor character of the dimer due to cooperative effects. The resultant hydrolysis was found to be activated with respect to the nonassisted mechanism, although it was difficult to isolate the effect of the pyramidalization and the effect of a favorable proton donation since the nucleophilic attack, the proton transfer, and amide bond cleavage were concerted in the mechanism.

To investigate the effect that a specific water-assisted proton transfer would have on the energetics of the species contributing to the reaction, we performed quantum mechanical calculations on the hydrolysis of formamide at a similar level of theory to the one used for the other species in this paper. In the earlier work of Bakowies et al.,[48] the MP2/6-31+G* level of theory was employed, and they found structures similar to the ones we report in this section. The intermediate in the hydrolysis of formamide and the transition state (TS2) for the breakdown of this intermediate were characterized at the B3LYP/6-31++G(d,p) level of theory. The analogue stationary points for the water-assisted mechanism were also determined. The geometries for these structures (INT_{OH2} and $TS2_{OH2}$) are depicted in Figure 7. The energy and effective energy barriers with solvation corrections of the transition states with respect to the intermediates are shown in Table 4 (with solvation corrections). Solvent contributions were introduced by single-point calculations at the B3LYP(PCM)/6-31++G(d,p) level of theory. To asses whether the TS2 transitions states were the stationary points connecting the intermediates and products, the intrinsic reaction coordinate[49,50] was followed as it departed from the two transition states. For each of the geometries along the IRC paths, we calculated the solvation free energy at the HF(PCM)/6-31G* level of theory to simplify the calculation. The results are shown in Figure 8.

TABLE 3: Comparing ΔG between the Hydrolysis of Pyramidal and Planar Amides[a]

molecule		gas phase	solution phase		
planar	pyramidal	$\Delta\Delta G_{gas}$	$\Delta\Delta G_{aq}^{PB-U}$	$\Delta\Delta G_{aq}^{PB-J}$	$\Delta\Delta G_{aq}^{PCM}$
$TS1_{chair}$	$TS1_{py}$	4.9	9.5	6.3	7.0
$TS1_{boat}$	$TS1_{py}$	8.2	12.6	9.3	9.7
INT_{chair}	INT_{py}	15.8	19.4	26.5	16.8
INT_{boat}	INT_{py}	19.2	23.1	25.2	18.2
$TS2_{chair}$	$TS2_{py}$	16.7	25.4	18.5	14.7
$PROD_{chair}$	$PROD_{py}$	22.5	24.5	26.2	22.8

[a] $\Delta\Delta G$ values defined as $\Delta G_{planar} - \Delta G_{pyramidal}$ in the gas phase and in aqueous solvent using PBU, PB-J, and PCM methods. (See Methods section.) All quantitaties are in kcal/mol.

TABLE 4: Barrier Relaxation for TS2 (in kcal/mol) Due to the Inclusion of an Explicit Water Molecule in the Calculations (Water-Assisted Mechanism)[a]

	no water-assisted	water-assisted	$\Delta\Delta E$
gas phase	13.0	7.4	5.7
solution	32.8	17.5	15.3

[a] Results were obtained at the B3LYP/6-31++G(d,p) level of theory for the hydrolysis of formamide. Barriers were calculated as the energy difference between TS2 and the intermediate INT (water-assisted) and between $TS2_{OH2}$ and INT_{OH2} (water-assisted). Solvation contributions were estimated by single-point B3LYP/6-31++G(d,p) energy evaluations at the gas-phase geometries.

The barrier for the non-water-assisted mechanism is 13.0 kcal/mol in the gas phase and 32.8 kcal/mol in solution. This is consistent with the trends we have observed for the hydrolysis of our pyramidal and planar amides, where the calculated barrier of TS2 with respect to that of INT is 14.4 kcal/mol in the gas phase and 30.0 kcal/mol in solution for the hydrolysis of the pyramidal amide and 10.3 kcal/mol in the gas phase and 27.1 kcal/mol in solution in the case of the hydrolysis of the planar amide: The PCM values of Table 2 were used, and the entropic contributions were removed so that the energies are comparable to those for formamide. The introduction of an explicit solvent water for the hydrolysis of formamide ($TS2_{OH2}$) lowers these barriers by a significant amount, as one can see from the IRC profiles of Figure 8 and the results of Table 4. The barriers are now 7.4 and 17.5 kcal/mol in the gas phase and in solution, respectively. This implies a relaxation of the barrier ($\Delta\Delta E$ in Table 4) of 5.7 kcal/mol in the gas phase and 15.3 kcal/mol in solution. Thus, proton transfer in the second step of the reaction is very sensitive to the influence of specific waters from the solvent, and it is likely that a bridging water molecule catalyzes the reaction by the facilitation of proton transfer. If this effect is included in the evaluation of the barriers for the second step of the reaction for the hydrolysis of the pyramidal and planar amides, then TS1 and TS2 would have more similar energies. Thus, in the case of the pyramidal amide, $TS1_{py}$ showed a free-energy barrier of 37.5 kcal/mol with respect to the reactant versus 51.0 kcal/mol for $TS2_{py}$. In the case of the planar amide, the differences were larger, 44.5 kcal/mol ($TS1_{chair}$) versus 65.7 kcal/mol ($TS2_{chair}$). After including the $\Delta\Delta E$ corrections of Table

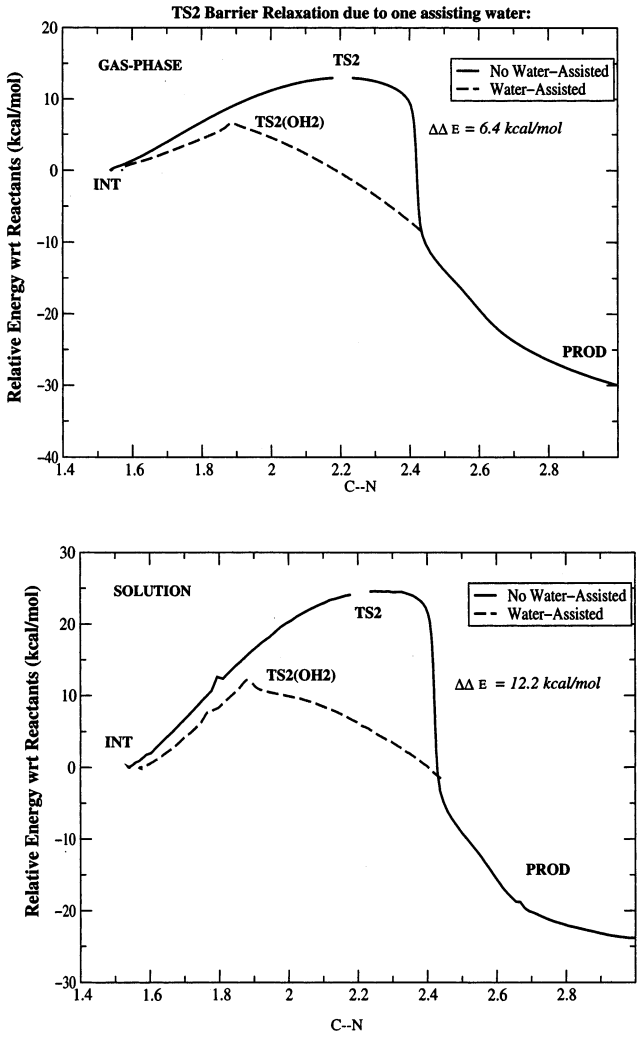

Figure 8. Reaction profiles for the breakdown of the intermediate in the hydrolysis of formamide. The IRC[49,50] pathways for the non-water-assisted mechanism (—) and the water-assisted mechanism (– –) are shown in the gas phase (top diagram) and in solution (bottom diagram). The pathway is shown as a function of the C−N bond distances obtained along the IRC and seems to suggest a sharp decrease in energy around a C−N value of 2.45 Å. The actual change in energy as a function of the IRC coordinate (combination of various degrees of freedom) is much smoother; therefore, the sharp decrease is a direct consequence of projecting the energy into one internal coordinate.

4, the energies for TS2 are reduced to 35.7 kcal/mol ($TS2_{py}$) and 50.4 kcal/mol ($TS2_{chair}$). It is important to note, however, that for the main purpose of this paper (i.e., characterization of the difference in barriers between the hydrolysis of a twisted amide and a planar amide) this effect is going to have only a minor influence since it would affect both reactions to a similar extent.

4. Discussion

In this section, we compare the differences in free energy between the hydrolysis of the twisted pyramidal and planar amides, and we relate the difference in free energy between the two reactions to electronic factors affecting the stability of the amide reactants (section 4.1). Then, we compare our estimates with the experimental evidence[7] of the acceleration of the hydrolysis of the pyramidal amides (section 4.2). To facilitate the discussion, we show in Table 3 the difference in ΔG ($\Delta\Delta G$) between analogue stationary points of the planar and pyramidal potential energy surfaces (e.g., the $\Delta\Delta G$ for TS1 is equal to $\Delta G^{TS1}_{planar} - \Delta G^{TS1}_{pyramidal}$).

4.1. Electronic Origin of Transition-State Stabilization. The values of $\Delta\Delta G$ are positive for all of the stationary points both in the gas phase and in solution with the continuum approximation (i.e., the hydrolysis of the twisted amide involves smaller barriers than the hydrolysis of the planar amide). Importantly, the values for $\Delta\Delta G$ found in solution are similar to the ones in the gas phase. This demonstrates that the faster hydrolysis of pyramidal amides results primarily from differential electronic effects present in the gas phase. Among them, the most relevant one, according to Glendening et al.,[42] is the absence of the $n_N \rightarrow \pi^*_{CO}$ stabilizing resonance in the twisted amide with a pyramidal conformation of the nitrogen.

To illustrate this effect, we consider the simplest amide, formamide (Figure 5). The ground state of formamide has a planar nitrogen (Figure 5A) corresponding to the partial double bond between N and C. Rotation around the C−N bond leads to a transition state (Figure 5B) in which the nitrogen now has a pyramidal conformation and where the resonance between the n_N lone pair and the $\pi^*_{C=O}$ orbital has been broken. As a consequence, longer C−N bond distances and shorter C−O distances are observed in the TS. These changes in bond lengths with the rotation of the C−N bond have been extensively analyzed by Wiberg et al.[35−40] The fact that the C−O bond length changes by an order of magnitude less than the C−N bond elongates has led[37,40−42] to a revision of the amide resonance model. However, a recent natural population analysis by Glendening et al.[42] has confirmed the important role of $n_N \rightarrow \pi^*_{CO}$ resonance in characterizing the ground-state electron density of planar formamide; they find natural resonant structures that are in agreement with the traditional $n_N \rightarrow \pi^*_{CO}$ resonance model. Therefore, our analysis is based on this type of model.

The rotation around the C−N bond in formamide shows an energy barrier of 20 kcal/mol at the B3LYP/6-311++G(d,p) level of theory. The barrier is not affected by solvent effects (i.e., when PCM contributions are included, a value of 20.6 kcal/mol is obtained). This value for the rotational barrier provided a measure of the stabilization energy of the $n_N \rightarrow \pi^*_{CO}$ resonance since the transition-state structure of formamide is very similar to the conformation adopted by the amide bond in the pyramidal reactant. This is nicely shown by an inspection of the values of τ and χ at the TS and the twisted amide reactant. (See Table 1.) The similarity of the value of these angles and the improper dihedrals also leads to the result that the amide bond and C−O bond distances do not change significantly.

We can also estimate the destabilization of the pyramidal reactant arising from the loss of the $n_N \rightarrow \pi^*_{CO}$ resonance by reducing the pyramidal and planar species to their formamide "equivalents". First, we take the conformation of the (C_5, C_6)−N−C_1−(O_1−C_2) atoms in the pyramidal amide reactant (see Figure 2), substitute C_2, C_5, and C_6 atoms with H, and relax the geometries with the constraint that the angles and dihedrals be kept the same as in the reactant. We do the same for the planar amide reactant (Figure 3), and we calculate the difference in energy between the two formamide structures. The result is 20.1 kcal/mol, a value very similar to the rotational barrier of formamide. These numbers also are very similar to the 23.0 kcal/mol resonance energy loss reported by Greenberg et al.[18] on the basis of differences in heats of formation for isodesmic processes in which amide is compared with its model amine and ketone components.

We now take the conformation of the (C_6, C_5)−N−C_1−(O_1, O_2H) skeleton of INT_{py} and $INT1_{chair}$ intermediates (see Figures 2 and 3), substitute C_2, C_5, and C_6 atoms with H, relax the geometries with frozen angles and dihedrals, and calculate the difference in energy between the two structures. The resulting difference in energy is only 0.6 kcal/mol, suggesting that there is no differential stability arising from the $n_N \rightarrow \pi^*_{CO}$ resonance when the intermediates are formed and the π_{CO} bond is broken.

If we consider the boat attack in the planar amide, which takes place on the face corresponding to the attack in the pyramidal amide, and look at the $\Delta\Delta G$ values of Table 3, then we see that the $\Delta\Delta G$ values in the gas phase are 8.2 and 19.2 kcal/mol for TS1 and the intermediate, respectively. This value of 19.2 kcal/mol is very close to the estimate of the stabilizing energy from the $n_N \rightarrow \pi^*_{CO}$ resonance discussed above. Thus, the results are coherent with the conclusion that the pyramidal amide reactant is destabilized relative to the planar amide by about 20.0 kcal/mol, and there is no resonance stabilization in either intermediate. In the TS1 transition state, a value for $\Delta\Delta G$ of 8.2 kcal/mol is obtained. This suggests that around 40% of the $n_N \rightarrow \pi^*_{CO}$ resonance has been lost in $TS1_{boat}$.

Since the chair attack leads to lower $\Delta\Delta G$ values than the boat attack, a reaction that passes through the chair conformation of the ring would be expected for the planar amide. The chair−boat stabilization is around 4.0 kcal/mol for the intermediate and 3.3 kcal/mol for TS1. The value of $\Delta\Delta G$ is 4.9 kcal/mol for $TS1_{chair}$ and 15.8 kcal/mol for the $INT1_{chair}$ intermediate. For TS2, a value of $\Delta\Delta G$ very similar to the one found for the intermediate, 16.7 kcal/mol, is obtained, and the $\Delta\Delta G$ of the product is augmented to 22.5 kcal/mol. These numbers can be understood from the fact that the $\Delta\Delta G$ values for the intermediates, TS2, and the product should reflect the 20.0 kcal/mol destabilization of the pyramidal amide reactant and, in addition, the 4.0 kcal/mol stabilization of the chair relative to the boat conformation of the ring.

4.2. Comparison with Experiment. Early kinetic work[7] suggested that a rate acceleration by a factor of 10^7 could be expected from the twist of the peptide bond and pyramidalization of nitrogen in amides under alkaline conditions. This corresponds to a barrier lowering of about 10.0 kcal/mol. Recent work by Kirby et al.[9,10] demonstrates even faster hydrolysis of highly twisted amides, though the conditions (i.e., pH) are different in the two sets of experiments. The observed rate acceleration in experiments is that of the overall rate of the reaction, inclusive of hydroxide attack and the breakdown of the tetrahedral intermediate. Depending on the relative free energies of TS1 and TS2, the relevant data to compare with the experimental $\Delta\Delta G^{\neq}$ is $\Delta\Delta G^{TS1}$ (when $\Delta G^{TS1} > \Delta G^{TS2}$) or $\Delta\Delta G^{TS2}$ (if $\Delta G^{TS2} > \Delta G^{TS1}$). As depicted in Table 3, $\Delta\Delta G^{TS1}$ is 6.3/7.0 kcal/mol (at PB-J/PCM) when we consider $TS1_{chair}$. This value increases to 9.3/9.7 kcal/mol if we compare $TS1_{boat}$ with $TS1_{py}$, structures that show an equivalent conformation of the lactam ring. The differential barrier for the second step of the reaction, $\Delta\Delta G^{TS2}$, is larger, 18.5/14.7 kcal/mol at PB-J/PCM levels of theory. On the basis of the data presented in Table 2, TS2 is higher than TS1 for the hydrolysis of the planar amide so that we would expect that the break in the resonance should account for 15.0−19.0 kcal/mol of barrier relaxation. However, we need to consider other aspects.

An analysis of multiple isotope effects[51,52] of the hydrolysis of formamide suggests that the breakdown of the anionic intermediate to the reactants or to the products involves TSs of similar energies. The discrepancy between this and our calculated relative energies of TS1 versus TS2 is a consequence of the use of our solvation model in which explicit waters that could assist in the proton transfer of the second step of the reaction are not included. To estimate this effect, we studied the simpler but closely related problem of the hydrolysis of formamide. This has been used as a model for peptide hydrolysis in several other studies.[13,14,48] In the case of formamide, the inclusion of an explicit water molecule results in a 15.3 kcal/mol reduction in the barrier. Using this for the pyramidal amide, the barrier for $TS2_{py}$ is estimated to be 35.7 kcal/mol (i.e., $\Delta G_{TS2_{py}} - 15.3$), a slightly lower barrier than $TS1_{py}$, which is 37.5 kcal/mol. In the case of the hydrolysis of the planar amide, the corrected barrier for TS2 ($\Delta G_{TS2chair} - 15.3$) is 50.4 kcal/mol, which is still higher than $TS1_{chair}$ (44.5 kcal/mol) but by only 6.0 kcal/mol. Additional explicit water molecules will probably decrease this number more, although the effect of a second water molecule is expected to be smaller than for the first addition. These results indicate that TS1 and TS2 have similar activation free energies, in agreement with the measured kinetic isotope effects. Applying the corresponding argument to the hydrolysis of the pyramidal amide that we have studied suggests that TS1 is the rate-limiting transition state for that reaction.

If the hydroxide attack is the rate-limiting step, then the experimental $\Delta\Delta G^{\neq}$ should be compared with $\Delta\Delta G^{TS1}$, and the agreement with the kinetic data of Blackburn[7] improves significantly, especially if one compares $TS1_{py}$ with $TS1_{boat}$, for which $\Delta\Delta G^{TS1}$ would have a value of 9.3/9.7 kcal/mol in solution and 8.2 kcal/mol in the gas phase. In summary, on the basis of kinetic isotope effects and the stabilizing effect of explicit water from our calculations for formamide, we believe that TS1 and TS2 will have similar energies in the case of the hydrolysis of a planar amide and that TS1 will be the rate-limiting step for the hydrolysis of the twisted amide. This leads to very good agreement between the theoretical $\Delta\Delta G^{TS1}$ and the experimental estimates for $\Delta\Delta G^{\neq}$ by Blackburn.[7]

The results of our calculation support and explain experimental data that indicate that a torsional distortion of an amide provides an effective means to accelerate the hydrolysis of the amide bond. However, the calculated barriers for the hydrolysis of the pyramidal amide are still higher than the fast acid-catalyzed hydrolysis of 1-aza-2-adamantanone observed by Kirby et al.[9,10] would suggest. Our calculations indicate that such a high rate of acceleration is unlikely to be a direct consequence of the breaking of resonance (i.e., the theoretical level captures the main electronic effects governing this type of acceleration). Another possibility is that the reaction of the twisted amide could involve an intrinsically different pathway. For instance, twisted and planar amides have very different gas-phase proton affinities, with a preference for N protonation for twisted amides and O protonation for planar amides.[18] This could lead to a different protonation state of the amide reactant when acidic media are involved. In fact, Brown et al. has estimated that the pK_a for distorted amides has values between 3.5 and 3.8,[2,8] showing that as the distortion decreases the pK_a's go toward the values of normal amides. In such a case, the barriers would be reduced not only by the effect of the loss of the π resonance but also by N protonation of the twisted amide, which is energetically unfavored for planar amides. Further calculations would be useful in determining the transition states of these other reaction pathways.

5. Conclusions

In this paper, we have studied how the rate acceleration observed in the hydrolysis of twisted amides is related to the

loss of the π resonance. To do so, we have characterized several intermediates, the key transition states, and products of the alkaline hydrolysis of a two closely related amides, one of which has a twisted amide bond and pyramidalized nitrogen in the reactant; the other has a normal planar amide bond. On the basis of the difference in the barriers for the pyramidal and planar systems of the two transition states for the reactions (TS1, corresponding to hydroxide attack, and TS2, corresponding to the breakdown of the intermediate), we conclude that $\Delta\Delta G^{\neq}$ values of 15.0−19.0 and 7.0−9.0 kcal/mol can be expected if TS2 and TS1 are the rate-limiting steps of the reaction, respectively. From kinetic isotope effect measurements and model studies of the effect of explicit solvent molecules on the mechanism of the analogous formamide hydrolysis, we conclude that TS1 and TS2 will have similar energies for the hydrolysis of the planar amide, whereas TS1 will be rate-limiting in the case of the hydrolysis of the pyramidal amide. If this is the case, then our estimation of the rate acceleration caused by the breakdown of π resonance in the reactant corresponds to a decrease in the barrier of 7.0−9.0 kcal/mol, in good agreement with early kinetic estimates of 10 kcal/mol by Blackburn et al.[7] The major contribution to the lowering of the barrier arises from the breaking of the π resonance, and the solvent effect is small. More recent observations of very fast hydrolysis of different reactions with twisted amides could have other origins; they will be the subject of a future publication.

Acknowledgment. This research was founded by the European Community Training and Mobility Research Program (COSSAC, ERBFMRXCT 980193 to X.L.). J.I. M. thanks Eusko Jaurlaritza for a grant.

References and Notes

(1) Brown, R.; Bennet, A.; Slebocka-Tilk, H. *Acc. Chem. Res.* **1992**, *25*, 482−488.

(2) Brown, R. Studies in Amide Hydrolysis: The Acid, Base, and Water Reactions. *The Amide Linkage: Selected Structural Aspects in Chemistry, Biochemistry and Materials Science*; Wiley & Sons: New York, 2000.

(3) Radzicka, A.; Wolfenden, R. *J. Am. Chem. Soc.* **1996**, *118*, 6105−6109.

(4) Krug, J.; Popelier, P.; Bader, R. *J. Phys. Chem.* **1992**, *96*, 7604−7616.

(5) Guthrie, J. *J. Am. Chem. Soc.* **1974**, *96*, 3608.

(6) Blackburn, G. M.; Plackett, J. D. *J. Chem. Soc., Perkin Trans. 2* **1972**, 1366−1371.

(7) Blackburn, G. M.; Skaife, C. J.; Kay, I. T. *J. Chem. Res.* **1980**, 294−295.

(8) Wang, Q.-P.; Bennet, A.; Brown, R.; Santarsiero, B. *J. Am. Chem. Soc.* **1991**, *113*, 5757−5765.

(9) Kirby, A. J.; Komarov, I. V.; Wothers, P.; Feeder, N. *Angew. Chem., Int. Ed.* **1998**, *37*, 785−786.

(10) Kirby, A. J.; Komarov, I. V.; Feeder, N. *J. Am. Chem. Soc.* **1998**, *120*, 7101−7102.

(11) Weiner, S. J.; Singh, U. C.; Kollman, P. *J. Am. Chem. Soc.* **1985**, *107*, 2219−2229.

(12) Hori, K.; Kamimura, A.; Ando, K.; Mizumura, M.; Ihara, Y. *Tetrahedron* **1997**, *53*, 4317−4330.

(13) Zheng, Y.-J.; Ornstein, R. L. *J. Mol. Struct.* **1998**, *429*, 41−48.

(14) Strajbl, M.; Florián, J.; Warshel, A. *J. Am. Chem. Soc.* **2000**, *122*, 5354−5366.

(15) Antonczak, S.; Ruiz-López, M. F.; Rivail, J. L. *J. Am. Chem. Soc.* **1994**, *116*, 3912−3921.

(16) Chalmet, S.; Harb, W.; Ruiz-López, M. F. *J. Phys. Chem. A* **2001**, *105*, 11574−11581.

(17) Greenberg, A.; Venanzi, C. A. *J. Am. Chem. Soc.* **1993**, *115*, 6951−6957.

(18) Greenberg, A.; Moore, D. T.; DuBois, T. D. *J. Am. Chem. Soc.* **1996**, *118*, 8658−8668.

(19) Davis, M. E.; Madura, J. D.; Luty, B. A.; McCammon, J. A. *Comput. Phys. Commun.* **1991**, *62*, 187−197.

(20) *Jaguar*, 3.5 ed.; Schrodinger, Inc.; Portland, OR, 1998.

(21) Frisch, M. J.; Trucks, G. W.; Schlegel, H. B.; Scuseria, G. E.; Robb, M. A.; Cheeseman, J. R.; Zakrzewski, V. G.; Montgomery, J. A., Jr.; Stratmann, R. E.; Burant, J. C.; Dapprich, S.; Millam, J. M.; Daniels, A. D.; Kudin, K. N.; Strain, M. C.; Farkas, O.; Tomasi, J.; Barone, V.; Cossi, M.; Cammi, R.; Mennucci, B.; Pomelli, C.; Adamo, C.; Clifford, S.; Ochterski, J.; Petersson, G. A.; Ayala, P. Y.; Cui, Q.; Morokuma, K.; Malick, D. K.; Rabuck, A. D.; Raghavachari, K.; Foresman, J. B.; Cioslowski, J.; Ortiz, J. V.; Stefanov, B. B.; Liu, G.; Liashenko, A.; Piskorz, P.; Komaromi, I.; Gomperts, R.; Martin, R. L.; Fox, D. J.; Keith, T.; Al-Laham, M. A.; Peng, C. Y.; Nanayakkara, A.; Gonzalez, C.; Challacombe, M.; Gill, P. M. W.; Johnson, B. G.; Chen, W.; Wong, M. W.; Andres, J. L.; Head-Gordon, M.; Replogle, E. S.; Pople, J. A. *Gaussian 98*, revision A.2; Gaussian, Inc.: Pittsburgh, PA, 1998.

(22) Gilli, G.; Bertolasi, V.; Belluccu, F.; Ferretti, V. *J. Am. Chem. Soc.* **1986**, *108*, 2420−2424.

(23) Ferretti, V.; Bertolasi, V.; Gilli, P.; Gilli, G. *J. Phys. Chem.* **1993**, *97*, 13568−13574.

(24) Becke, A. *Phys. Rev. A* **1988**, *38*, 3098.

(25) Lee, C.; Yang, W.; Parr, R. *Phys. Rev. B* **1988**, *37*, 785.

(26) Vosko, S. H.; Wilk, L.; Nusair, M. *Can. J. Phys.* **1980**, *58*, 1200.

(27) Becke, A. *J. Chem. Phys.* **1993**, *98*, 5648.

(28) Dobbs, K. D.; Dixon, D. A. *J. Phys. Chem.* **1996**, *100*, 3965−3973.

(29) Antonczak, S.; Ruiz-López, M. F.; Rivail, J. L. *J. Mol. Model.* **1997**, *3*, 434.

(30) Hehre, W.; Radom, L.; Schleyer, P.; Pople, J. *Ab Initio Molecular Orbital Theory*; Wiley-Interscience: New York, 1986.

(31) Cossi, M.; Barone, V.; Cammi, R.; Tomasi, J. *Chem. Phys. Lett.* **1996**, *225*, 327−335.

(32) Mineva, T.; Russo, N.; Sicilia, E. *J. Comput. Chem.* **1998**, *19*, 290−299.

(33) Barone, V.; Cossi, M.; Tomasi, J. *J. Chem. Phys.* **1997**, *107*, 3210−3221.

(34) York, D. M.; Karplus, M. *J. Phys. Chem. A* **1999**, *103*, 11060−11079.

(35) Wiberg, K.; Laidig, K. *J. Am. Chem. Soc.* **1987**, *109*, 5935.

(36) Wiberg, K.; Laidig, K. *J. Am. Chem. Soc.* **1992**, *114*, 831.

(37) Wiberg, K.; Hadad, C.; Rablen, P.; Cioslowski, J. *J. Am. Chem. Soc.* **1992**, *114*, 8644.

(38) Wiberg, K. B.; Rablen, P. R. *J. Am. Chem. Soc.* **1993**, *115*, 9234−9242.

(39) Wiberg, K. B.; Rablen, P. R. *J. Am. Chem. Soc.* **1995**, *117*, 2201−2209.

(40) Wiberg, K. B.; Rush, D. J. *J. Am. Chem. Soc.* **2001**, *123*, 2038−2046.

(41) Laidig, K. E.; Cameron, L. M. *J. Am. Chem. Soc.* **1996**, *118*, 1737−1742.

(42) Glendening, E. D.; Hrabal, J. A., II. *J. Am. Chem. Soc.* **1997**, *119*, 12940−12946.

(43) Reed, A. E.; Weinstock, R. B.; Weinhold, F. *J. Chem. Phys.* **1985**, *83*, 735−746.

(44) Glendening, E. D.; Badenhoop, J. K.; Weinhold, F. *J. Comput. Chem.* **1998**, *19*, 628−646.

(45) Chandrasekhar, J.; Smith, S.; Jorgensen, W. *J. Am. Chem. Soc.* **1985**, *107*, 154.

(46) Pearson, R. G. *J. Am. Chem. Soc.* **1986**, *108*, 6109−6114.

(47) Ford, G. P.; Wang, B. *J. Am. Chem. Soc.* **1992**, *114*, 10563−10569.

(48) Bakowies, D.; Kollman, P. A. *J. Am. Chem. Soc.* **1999**, *121*, 5712−5726.

(49) Gonzalez, C.; Schlegel, B. *J. Chem. Phys.* **1989**, *90*, 2154.

(50) Gonzalez, C.; Schlegel, B. *J. Phys. Chem.* **1990**, *94*, 5523−5527.

(51) Marlier, J. F.; Dopke, N. C.; Johnstone, K. R.; Wirdzig, T. J. *J. Am. Chem. Soc.* **1999**, *121*, 4356−4363.

(52) Marlier, J. F. *Acc. Chem. Res.* **2001**, *34*, 283−290.